Two-photon coherent control of femtosecond photoassociation

Christiane P. Koch,[1,*] Mamadou Ndong,[1] and Ronnie Kosloff[2]

[1] *Institut für Theoretische Physik, Freie Universität Berlin, Arnimallee 14, 14195 Berlin, Germany*

[2] *Department of Physical Chemistry and The Fritz Haber Research Center, The Hebrew University, Jerusalem 91904, Israel*

arXiv:0810.5738v1 [physics.atom-ph] 31 Oct 2008

Photoassociation with short laser pulses has been proposed as a technique to create ultracold ground state molecules. A broad-band excitation seems the natural choice to drive the series of excitation and deexcitation steps required to form a molecule in its vibronic ground state from two scattering atoms. First attempts at femtosecond photoassociation were, however, hampered by the requirement to eliminate the atomic excitation leading to trap depletion. On the other hand, molecular levels very close to the atomic transition are to be excited. The broad bandwidth of a femtosecond laser then appears to be rather an obstacle. To overcome the ostensible conflict of driving a narrow transition by a broad-band laser, we suggest a two-photon photoassociation scheme. In the weak-field regime, a spectral phase pattern can be employed to eliminate the atomic line. When the excitation is carried out by more than one photon, different pathways in the field can be interfered constructively or destructively. In the strong-field regime, a temporal phase can be applied to control dynamic Stark shifts. The atomic transition is suppressed by choosing a phase which keeps the levels out of resonance. We derive analytical solutions for atomic two-photon dark states in both the weak-field and strong-field regime. Two-photon excitation may thus pave the way toward coherent control of photoassociation. Ultimately, the success of such a scheme will depend on the details of the excited electronic states and transition dipole moments. We explore the possibility of two-photon femtosecond photoassociation for alkali and alkaline-earth metal dimers and present a detailed study for the example of calcium.

I. Introduction

Coherent control was conceived to solve the problem of optimizing the outcome of a chemical reaction[1,2]. Initial work was devoted to photodissociation[3,4]. In this study, we address the inverse problem of controlling the free-to-bound transition in photoassociation[5] where atoms are assembled to a molecule by laser light. The underlying principle of coherent control is interference of different pathways that lead from the initial state to the final outcome. Typically, in a free-to-bound transition, the relative phase between the reactants is not defined[1,6]: If the wavefunction of the

initial state can be written as a product of the wavefunctions of the atoms, the outcome of the binary reaction cannot be controlled. At very low temperatures, these considerations do not hold. Ultracold collisions are characterized by threshold effects[7,8]. The kinetic energy is very small, and the inner part of the scattering wavefunction is dominated by the potential energy. As a result, the colliding pair becomes entangled. Ultracold atoms are therefore the best candidates for coherent control of a binary reaction. The formation of molecules in ultracold atomic gases is presently attracting significant interest[9].

Previous proposals for short-pulse photoassociation were all based on one-photon transitions. Initially the goal was to optimize the excitation process in photoassociation by introducing a chirp[10,11]. In order to produce molecules in their ground electronic state, a pump-dump scheme was studied[12,13,14]: A first pulse excites two atoms and creates a molecular wave packet. This is followed by free dynamics on the electronically excited state bringing the wave packet to shorter internuclear distances. There a second pulse stabilizes the product by transferring amplitude to the ground electronic state. The pump-dump scheme can be supplemented by a third field to engineer the excited state wave packet dynamics to create favorable conditions for the dump pulse[15].

Experiments aiming at femtosecond photoassociation with a one-photon near-resonant excitation were faced with the obstacle that weakly bound molecular levels are very close to an atomic resonance. The challenge is to populate these levels without exciting the atomic transition. The weakly bound molecular levels possess the biggest free-bound Franck-Condon factors. However, the atomic transition matrix elements are several orders of magnitude larger. Excitation of the atomic transition is followed by spontaneous emission and trap loss, i.e. it leads to a depletion of the trap[16,17]. Pulses with bandwidths of a few wavenumbers corresponding to transform-limited pulse durations of a few picoseconds were proposed as a remedy[12,13]. However, for such narrow bandwidths, pulse shaping capabilities have yet to be developed. Experimenters employing femtosecond pulses with bandwidths of the order of $100\,\mathrm{cm}^{-1}$ have resorted to suppressing the spectral amplitude at the atomic resonance frequency by placing a razor knife into the Fourier plane of the pulse shaper[16,17,18]. Due to the finite spectral resolution, this leads also to the suppression of spectral amplitude which could excite the molecular levels with the largest free-bound Franck-Condon factors as illustrated in Fig. 1 (right-hand side). On the other hand, the spectral amplitude from the peak of the spectrum as well as from just below the cut finds almost no ground state population to excite since the probability of finding two colliding atoms at short internuclear distance is extremely small (left-hand side of Fig. 1). As a result, only a tiny part of the spectral amplitude contributes to the photoassociation signal[18].

Here we suggest to employ two-photon transitions for femtosecond photoassociation. The main idea consists in rendering the atomic transition dark by applying spectral or temporal phase control while exciting population into weakly bound molecular levels by two-photon transitions. The spectral resolution is determined by that of the pulse shaper, typically of the order of one wavenumber. This should allow for the population of weakly bound molecular levels with the best free-bound Franck-Condon factors.

Two-photon control is based on constructive or destructive interference of all two-photon pathways adding up to the two-photon transition frequency[19,20]. It allows for the excitation of a very narrow atomic transition by a broad band femtosecond pulse[19]. In particular, an anti-symmetric spectral phase optimizes non-resonant two-photon population transfer while a symmetric spectral phase yields a dark pulse[19]. For weak fields, the two-photon absorption yield can be calculated within perturbation theory, allowing for an analytical derivation of suitable phase functions. At intermediate fields, four-photon pathways additionally contribute to the two-photon absorption, requiring a higher order in the perturbation treatment[21,22]. In both the weak-field and intermediate-field regime, rational pulse shaping is based on frequency domain arguments[19,20,21,22]. For strong fields, a time-domain picture becomes more adequate since the dynamics are dominated by time-dependent Stark shifts[23,24,25]. The atom accumulates a phase due to the dynamic Stark shift. A suitable control strategy consists in eliminating this phase by applying a time-dependent phase function, i.e. by chirping the pulse[24]. This allows for maintaining a π-pulse condition despite the levels being strongly Stark shifted.

These results for coherent control of two-photon absorption in atomic systems serve as our starting point to derive pulses which are dark at the atomic transition but optimize two-photon photoassociation, i.e. population transfer into molecular levels. The shape of the pulses yielding a dark resonance of the atoms are derived analytically: In the weak-field and intermediate-field regimes, the two-photon spectrum is required to be zero at the atomic transition frequency, while for strong fields a time-dependent phase allows to maintain an effective 2π-pulse condition for the atoms. The shaped pulses are tested numerically for molecule formation. The paper is organized as follows: An effective two-state Hamiltonian is derived in Section II by adiabatically eliminating all off-resonant levels and invoking the two-photon rotating-wave approximation (RWA). In Section III, conditions for pulses that are dark at the two-photon atomic transition are derived analytically. Photoassociation is studied in Sections IV and V with Section IV reviewing possible two-photon excitation schemes for alkali and alkaline-earth dimers and Section V presenting the numerical study of two-photon photoassociation for calcium. Section VI concludes.

II. Theoretical framework for multi-photon excitations

We extend the treatment of multi-photon transitions in atoms[19,20,21,22,23,25] to include the vibrational degree of freedom, $\hat{\mathbf{R}}$, of a diatomic molecule. To this end, we write the nuclear Hamiltonian for each electronic state, $\hat{\mathbf{H}}_i = \hat{\mathbf{T}} + V_i(\hat{\mathbf{R}}) + \omega_i$ (setting $\hbar = 1$), i.e. all potentials, $V_i(\hat{\mathbf{R}})$, go to zero asymptotically and the atomic excitation energies are contained in ω_i. $\hat{\mathbf{T}}$ denotes the vibrational kinetic energy. Assuming the dipole approximation for the matter-field interaction, the total Hamiltonian is given by

$$\hat{\mathbf{H}} = \hat{\mathbf{H}}_0 + \hat{\boldsymbol{\mu}} E(t)\,, \tag{1}$$

where $\hat{\boldsymbol{\mu}}$ denotes the dipole operator and $E(t)$ the laser field with envelope $S(t)$, $E(t) = \frac{1}{2}E_0 S(t)\left(e^{\frac{i}{2}\varphi(t)}e^{-i\omega_L t} + c.c.\right)$. For weak and intermediate fields, the dynamics under the Hamiltonian, $\hat{\mathbf{H}}$, can be solved by perturbation theory. To lowest order, the two-photon absorption is given in terms of the two-photon spectral amplitude on resonance[19,20,21],

$$S_2 \sim \left| \int_{-\infty}^{+\infty} \tilde{E}(\omega_{ge}/2 + \omega)\tilde{E}(\omega_{ge}/2 - \omega)d\omega \right|^2, \tag{2}$$

where ω_{ge} is the two-photon resonance frequency and $\tilde{E}(\omega)$ the Fourier transform of $E(t)$. For an atomic system, conditions for a dark two-photon resonance are derived analytically by setting the integral to zero, see below in Section III A.

For strong fields, we follow the derivation of Trallero-Herrero et. al[23,25]. The matter Hamiltonian is expanded in the electronic basis, $|i\rangle\langle i|$,

$$\hat{\mathbf{H}}_0 = \sum_i \left(\hat{\mathbf{T}} + V_i(\hat{\mathbf{R}}) + \omega_i\right)|i\rangle\langle i|\,. \tag{3}$$

and the electronic states are separated into initial ground state, final excited state and intermediate states. If the one-photon detunings of the intermediate states, $\omega_{m,g/e} - \omega_L$, are large compared to the spectral bandwidth of the laser pulse, $\Delta\omega_L$, the intermediate states can be adiabatically eliminated[23]. Since the electronic excitation energies are much larger than the vibrational energies, the adiabatic elimination in the molecular model proceeds equivalently to the atomic case. Invoking a two-photon RWA, an effective two-state Hamiltonian is obtained,

$$\hat{\mathbf{H}}(t) = \begin{pmatrix} \hat{\mathbf{T}} + V_g(\hat{\mathbf{R}}) + \omega_g^S(t) & \chi(t)e^{-i\varphi(t)} \\ \chi(t)e^{i\varphi(t)} & \hat{\mathbf{T}} + V_e(\hat{\mathbf{R}}) + \Delta_{2P} + \omega_e^S(t) \end{pmatrix}, \tag{4}$$

where $\omega_{g/e}^S(t)$ denotes the dynamic Stark shift of the ground and excited state, $\chi(t)$ the two-photon coupling and Δ_{2P} the two-photon detuning, $\Delta_{2P} = \omega_{eg} - 2\omega_L$. The two-photon coupling is given

in terms of the one-photon couplings and one-photon detunings of the ground and excited state to the intermediate levels,

$$\chi(t) = -\frac{1}{4}E_0^2|S(t)|^2 \sum_m \frac{\mu_{em}\mu_{mg}}{\omega_{mg} - \omega_L}\,. \tag{5}$$

Similarly, the dynamic Stark shifts are obtained as

$$\omega_i^S(t) = -\frac{1}{2}E_0^2|S(t)|^2 \sum_m |\mu_{mi}|^2 \frac{\omega_{mi}}{\omega_{mi}^2 - \omega_L^2}\,, \quad i = g, e\,. \tag{6}$$

The transition dipole matrix elements, μ_{ij}, and the transitions frequencies, ω_{mi}, are in general R-dependent. They tend to a constant value (the atomic dipole moments and transition frequencies) at large internuclear distances that are important for photoassociation. The R-dependence is therefore neglected in the following.

Eqs. (5) and (6) contain couplings between the intermediate and the ground and excited states, but couplings between intermediate states are neglected. For very strong fields, these higher order couplings should be included. This type of adiabatic elimination is valid if the Stark shift is small relative to the energy spacing between the ground and excited states. The validity of the conditions for adiabatic elimination and two-photon RWA are easily checked in the atomic case by comparing the dynamics under the effective Hamiltonian, Eq. (4), to those under the full Hamiltonian, Eq. (1), including all intermediate levels. Possibly the Born-Oppenheimer potential energy surfaces in Eq. (3) show crossings or avoided crossings in the range of R that is addressed by the pulse. In such a case, Eq. (4) needs to be extended to include all coupled electronic states.

For strong-field control, it is instructive to choose the rotating frame such that the phase terms of the coupling in Eq. (4) are expressed as time-dependent frequencies [‡] and to time-dependently shift the origin of energy[23]. The transformed Hamiltonian is written,

$$\hat{\mathbf{H}}(t) = \begin{pmatrix} \hat{\mathbf{T}} + V_g(\hat{\mathbf{R}}) & \chi(t) \\ \chi(t) & \hat{\mathbf{T}} + V_e(\hat{\mathbf{R}}) + \left(\delta_\omega^S(t) + \Delta_{2P} + \dot{\varphi}\right) \end{pmatrix}, \tag{7}$$

where the differential Stark shift

$$\delta_\omega^S(t) = \omega_e^S(t) - \omega_g^S(t) \tag{8}$$

is introduced. In the atomic case, strong-field control consists in locking the phase corresponding to the term in parenthesis in Eq. (7), i.e. in keeping

$$\Phi(t) = \int_{-\infty}^{t} \delta_\omega^S(\tau)d\tau + \Delta_{2P}t + \varphi(t) \tag{9}$$

[‡] This corresponds to the fact that in the RWA a chirp can be expressed either as a phase term of the electric field envelope or as instantaneous laser frequency.

constant. This can be achieved by proper choice of phase of the laser pulse, $\varphi(t)$, and it corresponds to maintaining resonance by instantaneously correcting for the dynamic Stark shift[25].

III. Two-photon dark pulses

A. Solution in the weak- and intermediate-field regime

At low field intensities, the population transfer is dominated by the resonant two-photon pathways. Therefore control strategies are best understood in the frequency domain[21]. Starting from the Hamiltonian in the two-photon RWA, Eq. (4), the condition for a dark pulse at the atomic transition can be derived analytically. The atomic transition corresponds to the asymptotic limit of Eq. (4), i.e. to a two-level system. Since the two-photon coupling, $\chi(t)$, is proportional to the field amplitude squared, $E_0^2|S(t)|^2$, we look for a spectral phase such that the Fourier transform of $S(t)^2$,

$$F(\omega) = \int_{-\infty}^{+\infty} S^2(t) e^{i\omega t} dt = \int_{-\infty}^{+\infty} \tilde{S}(\omega')\tilde{S}(\omega - \omega') d\omega' \,,$$

becomes zero at the two-photon resonance, $F(\omega_{eg}) = 0$ ($\tilde{S}(\omega)$ is the Fourier transform of the envelope function $S(t)$). We assume a two-photon resonant pulse, $\omega_L = \omega_{eg}/2$. Then

$$\begin{aligned} F(\omega_{eg}) = 0 = F(2\omega_L) &= \int_{-\infty}^{+\infty} \tilde{S}(\omega')\tilde{S}(2\omega_L - \omega') d\omega' \\ &= \int_{-\infty}^{+\infty} \tilde{S}(\omega_L + \omega)\tilde{S}(\omega_L - \omega) d\omega \,. \end{aligned} \tag{10}$$

The condition in Eq. (10) is formally equivalent to that obtained in second order perturbation theory[19,21]. However, here we have derived it by considering the effective two-photon Hamiltonian, Eq. (4). The condition of Eq. (10) is sufficient for a two-photon dark pulse as long as the states are not strongly Stark-shifted, i.e. it holds also at intermediate field intensities. This finding is rationalized by considering the next order contribution. The fourth-order terms are classified into on-resonant and near-resonant terms[21]. The dominant fourth-order term is the one that includes the resonant second-order term and is therefore canceled by the same condition.

We assume the pulse shape to be Gaussian. Then $\tilde{S}(\omega) = A_0 e^{-\frac{(\omega-\omega_L)^2}{2\sigma_\omega^2}} e^{i\phi(\omega)}$ with σ_ω the spectral bandwidth, and the two-photon Fourier transform becomes

$$F(2\omega_L) = A_0^2 \int_{-\infty}^{+\infty} e^{-\frac{\omega^2}{\sigma_\omega^2}} e^{i\left(\phi(\omega_L+\omega)+\phi(\omega_L-\omega)\right)} d\omega \,.$$

We now need to choose the spectral phase $\phi(\omega)$ such as to render $F(2\omega_L)$ zero. This can be achieved by a step of the phase $\phi(\omega)$ by π[19,20].

We derive here the position of this step, ω_s. Let us assume that $\omega_s > \omega_L$, and denote $\Delta\omega_s = \omega_s - \omega_L$. Then

$$\phi(\omega_L+\omega)+\phi(\omega_L-\omega) = \begin{cases} 0 & \text{if} \quad \omega \geq \Delta\omega_s\,, \\ 0 & \text{if} \quad \omega \leq -\Delta\omega_s\,, \\ \pi & \text{if} \quad -\Delta\omega_s < \omega < \Delta\omega_s\,. \end{cases} \tag{11}$$

The π-step implies a change of sign in the integral, and the dark pulse condition is rewritten accordingly,

$$\begin{aligned} F(2\omega_L)/A_0^2 = 0 \;&=\; \int_{-\infty}^{-\Delta\omega_s} e^{-\frac{\omega^2}{\sigma_\omega^2}}\,d\omega + \int_{\Delta\omega_s}^{+\infty} e^{-\frac{\omega^2}{\sigma_\omega^2}}\,d\omega - \int_{-\Delta\omega_s}^{\Delta\omega_s} e^{-\frac{\omega^2}{\sigma_\omega^2}}\,d\omega\,, \\ &=\; 2\int_{\Delta\omega_s}^{+\infty} e^{-\frac{\omega^2}{\sigma_\omega^2}}\,d\omega - 2\int_{0}^{\Delta\omega_s} e^{-\frac{\omega^2}{\sigma_\omega^2}}\,d\omega\,. \end{aligned}$$

We recognize the error function up to a factor and obtain

$$\mathsf{Erf}\left(\frac{\Delta\omega_s}{\sigma_\omega}\right) = \frac{1}{2}\,, \tag{12}$$

which determines $\Delta\omega_s$ and hence the step position, ω_s. That is, if one chooses $\Delta\omega_s$ such that $\mathsf{Erf}(\sigma\Delta\omega_s) = 1/2$, the two-photon spectrum is zero at the two-photon transition frequency, $F(2\omega_L) = 0$, and a dark pulse is obtained. Interestingly we can also combine the conditions of a symmetrical function and a phase step. This is achieved by defining two phase steps symmetrical around ω_L, $\omega_L \pm \omega_s$. Following a derivation along the same lines as outlined above, the identical condition for ω_s is obtained.

B. Solution in the strong-field regime

At high intensities, the effective Hamiltonian varies during the pulse. A time-domain picture is therefore best adapted to develop control strategies. Population inversion in the effective Hamiltonian can be achieved by adjusting the temporal phase of the laser such as to maintain a π-pulse condition[23,24]. Here we turn this strategy upside-down to achieve a dark pulse, i.e. we ask for the 2π-pulse condition. We restrict the notation to the atomic case for simplicity. The Hamiltonian, Eq. (7), can be transformed such that the diagonal elements are zero[25],

$$\hat{\mathbf{H}}(t) = \begin{pmatrix} 0 & \chi(t)e^{-i\Phi(t)} \\ \chi(t)e^{i\Phi(t)} & 0 \end{pmatrix}. \tag{13}$$

Evaluating Rabi's formula for the final state amplitude leads to the condition

$$\left|\int_0^{t_f} \chi(t)e^{i\Phi(t)}dt\right| = 2k\pi\,, \quad k = 0, 1, \ldots \tag{14}$$

for zero population transfer to the excited state. We again assume a two-photon resonant pulse, $\omega_{ge} = 2\omega_L$. The condition, Eq. (14), is fulfilled given the phase $\Phi(t)$ obeys

$$\Phi(t) = \begin{cases} \pi & \text{if} \quad t_0 - \Delta t_x < t < t_0 + \Delta t_x \,, \\ 0 & \text{elsewhere} \,. \end{cases} \tag{15}$$

This corresponds to the following temporal laser phase

$$\varphi(t) = \begin{cases} -\pi - \int_0^t \delta_\omega^S(\tau) d\tau & \text{if} \quad t_0 - \Delta t_x < t < t_0 + \Delta t_x \\ -\int_0^t \delta_\omega^S(\tau) d\tau & \text{elsewhere} \end{cases} \tag{16}$$

For a Gaussian pulse, the time-dependence of the differential Stark shift is also Gaussian, and $\varphi(t)$ can be evaluated analytically. Inserting the definition of $\Phi(t)$, Eq. (9), into the condition, Eq. (14), and evaluating the integrals yields a condition for Δt_x,

$$\mathsf{Erf}\left(\frac{\Delta t_x}{\sigma}\right) = \frac{1}{2} \,. \tag{17}$$

A pulse with the temporal phase defined by Eqs. (16) and (17) suppresses population transfer by keeping the two levels out of resonance.

Such a solution can also be obtained by applying local control[26] to the effective Hamiltonian, Eq. (13). Local control theory allows to carry the analysis over to the full molecular problem. We can seek conditions which eliminate atomic two-photon transitions while maximizing the molecular population transfer. To this end, we define an operator to be minimized,

$$\hat{\mathbf{P}}_{at} = \int_{R_0}^{+\infty} dR |e\rangle\langle e| \,, \tag{18}$$

which projects onto the atomic levels, $|e\rangle$ denotes the excited electronic state. R_0 is a distance which is larger than the bond length of the last bound level of the excited state potential. The objective to be maximized is defined by the projection onto the molecular levels for photoassociation,

$$\hat{\mathbf{P}}_{mol} = \sum_i |\varphi_i^e\rangle\langle\varphi_i^e| \,, \tag{19}$$

where $|\varphi_i^e\rangle$ denote vibrational eigenstates of the electronically excited state. In local control theory, we seek the phase of the field such that

$$\frac{d}{dt}\langle\hat{\mathbf{P}}_{at}\rangle = 0 \qquad \frac{d}{dt}\langle\hat{\mathbf{P}}_{mol}\rangle > 0 \,, \tag{20}$$

i.e. atomic transitions are suppressed while the molecular population is monotonically increasing[27]. Eq. (16) is a specific analytical example of local control. The first part of the pulse up to time

$t \leq t_0 - \Delta t_x$ builds up excited state population and a phase relation between the ground and excited levels. At this instant in time the phase of the field jumps by π so that it becomes perpendicular to the phase of the instantaneous transition dipole, thus eliminating additional population transfer. The last part of the pulse restores the original population.

IV. Two-photon excitation schemes for photoassociation

Our goal is to populate molecular levels in a long-range potential while suppressing excitation of the atomic transition. We will restrict the discussion to homonuclear dimers where potentials with $1/R^5$ behavior occur below the $S + D$ asymptote* . In heteronuclear dimers, the potentials go as $1/R^6$, and the improvement of two-photon over one-photon femtosecond photoassociation is expected to be less significant. Alkali and alkaline earth species where cooling and trapping of atoms is well established are considered. Carrier frequencies in the near-infrared are assumed throughout.

A. Two-photon transitions in alkali dimers

A one-photon transition cannot be controlled by interference between different photon pathways. A prerequisite for our scheme is therefore that no one-photon resonances be contained within the pulse spectral bandwidth. This excludes both potassium and rubidium as possible candidates. Of the remaining alkalis, only caesium shows a two-photon resonance between the ground state and a d-level in the near-infrared, cf. Table I.

B. Two-photon transitions in alkaline earth dimers

Of the alkaline earth atoms, calcium and strontium show two-photon resonances at the desired wavelength, cf. Table I, and in magnesium a near-IR four-photon transition to a d level is possible. In the following we will study calcium since potential curves for a large number of electronically excited states are known with sufficient accuracy[28].† The two-photon excitation scheme is shown

* One may also consider transitions into potentials correlating to an $S + P$ asymptote. While this is two-photon forbidden for atoms, it might be two-photon allowed at short internuclear distances. However, in that case photoassociation will occur only at distances below 20 Bohr. This corresponds to large detunings, and a two-photon control scheme is then not required.

† We expect that our reasoning can be carried over to strontium with only slight modifications due to the similar electronic structure.

in Fig. 2: Two atoms interacting via the $X^1\Sigma_g^+$-state are excited into bound levels of the $(1)^1\Pi_g$-state or the $(2)^1\Sigma_g^+$-state that both correlate to the $^1S + ^1D$ asymptote. Note that the ^1D term of calcium occurs energetically below the $^1P^0$ term. The dipole coupling is provided by the states with one-photon allowed transitions from the ground state, i.e. the $A^1\Sigma_u^+$, $A'^1\Pi_u$, $B^1\Sigma_u^+$ states and further electronic states at higher energies. The effective two-photon coupling, cf. Eq. (5), is determined by the dipole matrix elements of the one-photon allowed transitions and by the one-photon detunings. Compared to the atomic two-photon transitions studied in caesium[19] and sodium[21,22,24,25], the one-photon detunings in the alkaline earths are much larger. Higher laser intensities will therefore be required.

Fig. 3 demonstrates the existence of long-range vibrational wavefunctions in a potential with $1/R^5$ behavior for large internuclear distances R. Vibrational wavefunctions of the $(1)^1\Pi_g$ excited state potential are plotted in Fig. 3a for three different binding energies. The wavefunctions need to be compared to the initial scattering state, shown in Fig. 3b for two ground state atoms colliding with approximately $40\,\mu$K: Large free-bound Franck-Condon factors are due to sufficient probability density at large R in the excited state vibrational wavefunctions. In the following population shall be transferred from the initial ground state atomic density into these vibrational wavefunctions close to the excited-state dissociation limit. The efficiency will be determined by the width of the dark atomic resonance, i.e. by how close to the dissociation limit excitation into molecular levels can occur.

V. Two-photon photoassociation in calcium

Photoassociation of two calcium atoms is studied by numerically solving the time-dependent Schrödinger equation for the effective two-photon Hamiltonian, Eq. (4), with a Chebychev propagator[29]. The Hamiltonian is represented on a grid using an adaptive grid step size[30,31,32]. The two-photon couplings and dynamic Stark shifts are calculated from the atomic transition dipole matrix elements and frequencies found in Ref.[33]. The potentials are gathered from Ref.[28]. An initial state with a scattering energy corresponding to $40\,\mu$K, cf. Fig. 3b, is chosen.

Fig. 4 presents calculations with transform-limited pulses of 100 fs full-width half-maximum and a central wavelength of 915 nm. They serve as reference point for the shaped pulse calculations discussed below. Fig. 4a shows the final excited state population including both atoms and molecules as a function of pulse energy. The arrows in Fig. 4a indicate pulse energies in the weak, intermediate and strong field regime that are employed in shaped pulse calculations. Rabi

oscillations are observed as the pulse energy is increased. The contrast of the oscillations is reduced from 100% to 14%. This is a clear sign of the dynamic Stark shift for strong fields. For strong (intermediate) field, the maximum Stark shift, Eq. (6), amounts to $104\,\mathrm{cm}^{-1}$ ($32\,\mathrm{cm}^{-1}$) for the ground state and to $247\,\mathrm{cm}^{-1}$ ($76\,\mathrm{cm}^{-1}$) for the excited state. The weak field corresponds to a pulse energy of $0.94\,\mu$J and yields an excited state population of 5.0×10^{-3}, the intermediate field to $2.4\,\mu$J and $P_{exc}(t_{final}) = 2.9\times10^{-2}$, and the strong field to $7.6\,\mu$J and $P_{exc}(t_{final}) = 1.4\times10^{-1}$.

The projection of the final wave packet onto the molecular levels of the excited state, i.e. the excited state vibrational distribution after the pulse, is shown in Fig. 4b for transform-limited two-photon π and 2π-pulses. For a π-pulse, the population of the last bound level amounts to 1.8×10^{-3} compared to an atomic population of 1.4×10^{-1}. For comparison, one-photon photoassociation with a 10 ps-pulse detuned by $4\,\mathrm{cm}^{-1}$ achieves a population transfer into molecular levels on the order of 10^{-4} which corresponds, depending on the trap conditions, to 1-10 molecules per pulse[13,14]. The arrows in Fig. 4b indicate the binding energies of a few weakly bound levels. Due to their smaller free-bound Franck-Condon factors, deeper molecular levels are populated significantly less than the last bound level. The minimum of the excited state vibrational distribution at $v=-4$ is due to the node of the scattering wavefunction at $R\sim68\,\mathrm{a}_0$, cf. Fig. 3b.

Frequency-domain control is studied for weak and intermediate fields in Fig. 5. The shaped pulses are obtained by applying a spectral phase function consisting of a π-step to a transform-limited 100 fs-pulse, cf. Eq. (11). The position of the π-step is varied. Atomic population transfer (black filled circles) can be strongly suppressed, by 10^{-6}, for the weak field, see Fig. 5a. For the intermediate field, Fig. 5b, the dynamic Stark shift moves the levels during the pulse. The dark-pulse condition taking into account only the static resonance frequency, Eq. (10), is then not sufficient anymore to strongly suppress atomic population transfer. The maximum suppression, i.e. the minimum of the final excited state population, is therefore reduced to be on the order of 10^{-3}. It is observed at the position of the π-step corresponding to Eq. (12), detuned by $42.2\,\mathrm{cm}^{-1}$ from the carrier frequency for both weak and intermediate field.

When population transfer into all molecular levels is considered, no difference between atoms and molecules is observed, compare the black filled circles and open green squares in Fig. 5. In this case the last two levels which have the largest free-bound Franck-Condon factors dominate the molecular population transfer. Since their binding energy is very small, less than $0.01\,\mathrm{cm}^{-1}$, there is almost no detuning with respect to the atomic two-photon resonance, and the dark-state condition applies to the atomic transition and transitions into the last two bound levels alike. As the binding energy of the molecular levels and hence the detuning from the atomic resonance

increases, the two-photon dark state condition which is defined at the atomic resonance becomes less applicable. Subsequently, molecular two-photon transitions become less dark, cf. open triangles and diamonds in Fig. 5. Atomic transitions are suppressed by about four orders of magnitude more then transitions into molecular levels with binding energies larger than $1\,\mathrm{cm}^{-1}$ for the weak field. This needs to be compared to the difference in atomic and molecular transition matrix elements. For weakly bound levels, it amounts to four to five orders of magnitude. The suppression of the atomic transition in Fig. 5a implies therefore that about the same number of atoms and of molecules bound by more than $1\,\mathrm{cm}^{-1}$ will be excited. The excited atoms will be lost. However, this loss is sufficiently small, and the trap is not depleted. Due to the high repetition rate in femtosecond experiments, many photoassociation pulses can be applied before any significant depletion of the trap occurs. At intermediate field strength, the atomic transition relative to transitions into molecular levels with binding energies larger than $1\,\mathrm{cm}^{-1}$ is suppressed by only two orders of magnitude. In that case, loss of atoms from the trap becomes significant, and the control strategy of applying a spectral π-step phase function is not sufficient to accumulate molecules by applying many photoassociation pulses.

For intermediate and strong fields, pulse shaping in the time-domain is more appropriate since it allows to correct for the dynamic Stark shift. Time-domain control is studied in Fig. 6. The shaped pulses are obtained by chirping the pulse according to Eq. (16) with the chirp time interval, Δt_x, determined from Eq. (17). The final excited state population, normalized with respect to the transform limited case, is compared for atoms and molecules in Fig. 6 for intermediate (a) and strong (b) fields. It is plotted for increasing duration of the transform-limited pulse from which the chirped pulse is generated, keeping the pulse energy constant. For time-domain control, two-photon transitions for atoms are clearly more strongly suppressed than for molecules. The ratio of suppression of atoms versus molecules varies as a function of the transform-limited pulse duration between one and five orders of magnitude demonstrating a large amount of control. The overall increase of the difference between atoms and molecules with increasing pulse duration is rationalized in terms of the control strategy: The dynamic Stark shift together with the two-photon detuning leads to the accumulation of a phase in the atoms and molecules. It is countered by the laser phase $\varphi(t)$, cf. Eq. (9). The difference between atoms and molecules becomes more perceptible for longer phase accumulation times. The modulations seem to be caused by a periodic accumulated phase of the instantaneous transition dipole. More analysis using local control theory is required. Overall, however, the suppression of the molecular transitions is much too strong to achieve any significant photoassociation yield. Analysing the molecular transitions for the weakly bound levels relevant

in photoassociation, no dependence on binding energy is observed. Transitions into levels bound by $1\,\mathrm{cm}^{-1}$ or more are equally suppressed as transitions into the last two bound levels. This is not surprising since the levels have a very similar dynamic Stark shift. Differences arise mostly from the different two-photon detunings, and they are much smaller than the dynamic Stark shift. It is hence not enough to enforce a minimization of the atomic transition probability. The molecular transition probabilities need to be maximized explicitly, e.g. employing local control and Eq. (20).

VI. Summary and conclusions

We have studied coherent control of femtosecond photoassociation employing two-photon transitions. The goal of our study was to identify pulses which populate molecular levels close to the atomic transition without exciting the atoms themselves. An effective two-photon Hamiltonian was derived by extending previous work on atoms[23,24] by the vibrational degree of freedom. In the weak-field to intermediate-field regime, frequency-domain control was pursued based on applying a spectral phase function. This leads to constructive or destructive interference between all pathways contributing to the two-photon absorption[19,20,21,22]. Time-domain control is more appropriate for the intermediate-field to strong-field regime where the dynamics are dominated by dynamic Stark shifts[23,24]. A temporal phase function allows to lock the atomic phase to that of the laser, keeping the atoms on or out of resonance. For both regimes, we derived analytical conditions to construct pulses which leave the atomic two-photon transition dark. These pulses were tested in a numerical study of photoassociation in calcium. An excited-state potential correlating to the $^1S + ^1D$ asymptote was chosen. It shows a $1/R^5$ behavior at long range and supports weakly bound molecular levels with large free-bound Franck-Condon factors required for efficient photoassociation.

In the weak-field regime, applying a π-phase step reduces the atomic transition probability by a factor of 10^{-6}. Molecular levels with binding energies of about $1\,\mathrm{cm}^{-1}$ are sufficiently detuned from the atomic two-photon resonance that the dark condition does not apply. Transitions into these levels are suppressed by only a factor of 10^{-2}. The resulting four orders of magnitude difference between atomic and molecular transitions is sufficient to counter the different excitation probabilities for atoms and molecular levels. It hence allows for employing femtosecond pulses without depleting the trap due to excitation of atoms. However, weak-field control implies that absolute excitation probabilities are very small.

In the intermediate-field regime, the Stark shift becomes large enough to move the levels during the pulse. The spectral dark pulse condition taking into account only the static two-photon

resonance is then not sufficient to suppress atomic transitions. A reduction of the atomic transition probability by merely a factor of 10^{-3} was found. Applying a femtosecond pulse will then excite significantly more atoms than molecules. Since the excited atoms are lost, trap depletion is expected to set in after a few pulse cycles.

Time-domain control based on maintaining a 2π-pulse condition for the atomic transition is applicable for both intermediate and strong fields. The ratio of suppression of atomic versus molecular transitions depends on the duration of the transform-limited pulses from which the shaped pulses are generated. It reaches up to five orders of magnitude. This finding is rationalized in terms of accumulation of different phases for atoms and molecules. In absolute numbers, however, the molecular transitions themselves are strongly suppressed. A significant photoassociation yield can therefore not be achieved by the simple control strategy based on the analytical result for the atomic two-photon excitation. Local control should be employed to maximize the molecular transition probabilities while keeping the atomic line dark. This is beyond the scope of the present study.

In conclusion, an impressive amount of control yielding several orders of magnitude difference between atomic and molecular transitions could be demonstrated with both spectral and temporal phase shaping. However, the two-photon photoassociation efficiencies need to be improved in terms of absolute numbers of molecules per pulse to yield a feasible photoassociation scheme. In the strong-field regime, local control offers a means for explicit maximization of molecular transition probabilities. Moreover, our discussion could be extended from two-photon to three-photon transitions. Then, excited-state potentials correlating to $S + P$ asymptotes and showing a $1/R^3$ behavior at long range could be employed. A $1/R^3$ long-range potential supports spatially more extended vibrational wavefunctions than a $1/R^5$ potential and exhibits an overall larger density of vibrational levels. Therefore, the efficiency of a shaped pulse which allows to excite weakly bound molecular levels in a three-photon transition while keeping the atomic resonance dark is expected to by far exceed that of the two-photon scheme.

Acknowledgements

We wish to thank Zohar Amitay and Yaron Silberberg for fruitful discussions. Financial support from the Deutsche Forschungsgemeinschaft through the Emmy Noether programme and SFB 450 is gratefully acknowledged.

* Electronic address: ckoch@physik.fu-berlin.de

[1] P. Brumer and M. Shapiro, *Principles and Applications of the Quantum Control of Molecular Processes*, Wiley Interscience, 2003.

[2] S. A. Rice and M. Zhao, *Optical control of molecular dynamics*, John Wiley & Sons, New York, 2000.

[3] T. Baumert, B. Bühler, R. Thalweiser, and G. Gerber, *Phys. Rev. Lett.*, 1990, **64**(7), 733–736.

[4] V. D. Kleiman, L. Zhu, J. Allen, and R. J. Gordon, *J. Chem. Phys.*, 1995, **103**(24), 10800–10803.

[5] K. M. Jones, E. Tiesinga, P. D. Lett, and P. S. Julienne, *Rev. Mod. Phys.*, 2006, **78**, 483.

[6] C. A. Arango, M. Shapiro, and P. Brumer, *J. Chem. Phys.*, 2006, **125**, 094315.

[7] J. Weiner, V. S. Bagnato, S. Zilio, and P. S. Julienne, *Rev. Mod. Phys.*, 1998, **71**(1), 1–85.

[8] F. Masnou-Seeuws and P. Pillet, *Adv. in At., Mol. and Opt. Phys.*, 2001, **47**, 53–127.

[9] J. M. Hutson and P. Soldan, *Int. Rev. Phys. Chem.*, 2006, **25**(4), 497–526.

[10] J. Vala, O. Dulieu, F. Masnou-Seeuws, P. Pillet, and R. Kosloff, *Phys. Rev. A*, 2000, **63**, 013412.

[11] E. Luc-Koenig, R. Kosloff, F. Masnou-Seeuws, and M. Vatasescu, *Phys. Rev. A*, 2004, **70**, 033414.

[12] C. P. Koch, E. Luc-Koenig, and F. Masnou-Seeuws, *Phys. Rev. A*, 2006, **73**, 033408.

[13] C. P. Koch, R. Kosloff, and F. Masnou-Seeuws, *Phys. Rev. A*, 2006, **73**, 043409.

[14] C. P. Koch, R. Kosloff, E. Luc-Koenig, F. Masnou-Seeuws, and A. Crubellier, *J. Phys. B*, 2006, **39**, S1017.

[15] C. P. Koch and R. Moszyński, *Phys. Rev. A*, 2008, **78**, xxx.

[16] W. Salzmann, U. Poschinger, R. Wester, M. Weidemüller, A. Merli, S. M. Weber, F. Sauer, M. Plewicki, F. Weise, A. Mirabal Esparza, L. Wöste, and A. Lindinger, *Phys. Rev. A*, 2006, **73**, 023414.

[17] B. L. Brown, A. J. Dicks, and I. A. Walmsley, *Phys. Rev. Lett.*, 2006, **96**, 173002.

[18] W. Salzmann, T. Mullins, J. Eng, M. Albert, R. Wester, M. Weidemüller, A. Merli, S. M. Weber, F. Sauer, M. Plewicki, F. Weise, L. Wöste, and A. Lindinger, *Phys. Rev. Lett.*, 2008, **100**, 233003.

[19] D. Meshulach and Y. Silberberg, *Nature*, 1998, **396**, 239–242.

[20] D. Meshulach and Y. Silberberg, *Phys. Rev. A*, 1999, **60**(2), 1287.

[21] L. Chuntonov, L. Rybak, A. Gandman, and Z. Amitay, *Phys. Rev. A*, 2008, **77**, 021403.

[22] L. Chuntonov, L. Rybak, A. Gandman, and Z. Amitay, *J. Phys. B*, 2008, **41**(3), 035504 (11pp).

[23] C. Trallero-Herrero, D. Cardoza, T. C. Weinacht, and J. L. Cohen, *Phys. Rev. A*, 2005, **71**, 013423.

[24] C. Trallero-Herrero, J. L. Cohen, and T. Weinacht, *Phys. Rev. Lett.*, 2006, **96**, 063603.

[25] C. Trallero-Herrero and T. C. Weinacht, *Phys. Rev. A*, 2007, **75**, 063401.

[26] R. Kosloff, A. D. Hammerich, and D. Tannor, *Phys. Rev. Lett.*, 1992, **69**(15), 2172–2175.

[27] A. Bartana, R. Kosloff, and D. J. Tannor, *J. Chem. Phys.*, 1993, **99**(1), 196–210.

[28] B. Bussery-Honvault and R. Moszynski, *Mol. Phys.*, 2006, **104**(13-14), 2387–2402.

[29] R. Kosloff, *Annu. Rev. Phys. Chem.*, 1994, **45**, 145–178.

[30] V. Kokoouline, O. Dulieu, R. Kosloff, and F. Masnou-Seeuws, *J. Chem. Phys.*, 1999, **110**, 9865.

[31] K. Willner, O. Dulieu, and F. Masnou-Seeuws, *J. Chem. Phys.*, 2004, **120**, 548.

[32] S. Kallush and R. Kosloff, *Chem. Phys. Lett.*, 2006, **433**(1-3), 221.

[33] NIST Atomic Spectra Database, http://physics.nist.gov/PhysRefData/ASD.

atom	transition	wavelength
Cs	$6s \rightarrow 7d$	$2 \times 768\,\mathrm{nm}$
Mg	$3s^2 \rightarrow 3s3d$	$4 \times 862\,\mathrm{nm}$
Ca	$4s^2 \rightarrow 3d4s$	$2 \times 915\,\mathrm{nm}$
Sr	$5s^2 \rightarrow 4d5s$	$2 \times 992\,\mathrm{nm}$

TABLE I: Two-photon transitions which are candidates for two-photon photoassociation in the near-infrared for alkali and alkaline earth atoms

Fig. 1 In one-photon photoassociation, blocking the spectral amplitudes at and close to the atomic resonance prevents weakly bound molecular levels with large free-bound Franck-Condon factors to be excited (right-hand side). The majority of spectral components does not find any ground state population to be excited since the probability to find two colliding atoms at short internuclear distance is tiny (left-hand side, data shown here for Rb_2). In femtosecond photoassociation employing a one-photon transition, the large majority of spectral components passes through the sample without any effect.

Fig. 2 Two-photon photoassociation of two atoms colliding over the $X^1\Sigma_g^+$ ground state into the $(1)^1\Pi_g$-state or the $(2)^1\Sigma_g^+$-state correlating to the $s+d$ asymptote (solid lines). The dipole coupling is provided by the states with one-photon allowed transitions from the ground state such as the $A^1\Sigma_u^+$-state or the $B^1\Sigma_u^+$-state (dashed lines). The example shown here is Ca_2.

Fig. 3 Weakly bound vibrational wavefunctions of the $(1)^1\Pi_g$ excited state for three different binding energies relevant for photoassociation (a) and scattering wavefunction of two ground state calcium atoms (b).

Fig. 4 (a) The excited state population shows Rabi oscillations as the pulse energy is increased. The arrows indicate the pulsed energies which are employed for shaped pulses. (b) The projection of the final excited state wave packet onto the molecular levels, i.e. the excited state vibrational distribution after the pulse for a two-photon π-pulse and a two-photon 2π-pulse. The arrows indicate the range of binding energies relevant in the discussion of the results for shaped pulses.

Fig. 5 Frequency-domain control with pulses shaped according to Eq. (11): The excited state population of atoms (filled circles) and of molecules (open symbols), normalized with respect to the results obtained for a transform-limited pulse, is shown as a function of the π-step position for (a) weak and (b) intermediate fields. Population transfer can be strongly suppressed, by 10^{-6}, for the weak field (a). For the intermediate field (b), the dynamic Stark shift sets in yielding a maximum suppression on the order of 10^{-3}. When all molecular levels are considered, the last two levels (that have binding energies of less than $0.01\,\mathrm{cm}^{-1}$) dominate and no difference between atoms and molecules is observed. For increasing binding energy of the molecular levels, and hence detuning from the atomic resonance, the two-photon transition becomes less dark.

Fig. 6 Time-domain control with pulses shaped according to Eq. (16): The excited state population of atoms (filled circles) and of molecules (open symbols), normalized with respect to the results obtained for a transform-limited pulse, is shown as a function of the duration of the corresponding transform-limited pulse for intermediate (a) and strong field (b). Two-photon transitions for atoms are more strongly suppressed than for molecules. However, the suppression of the molecular transitions is too strong to achieve any significant photoassociation yield. For weakly bound levels no difference in the suppression with increasing binding energy is observed, i.e. the levels have very similar dynamic Stark shifts.

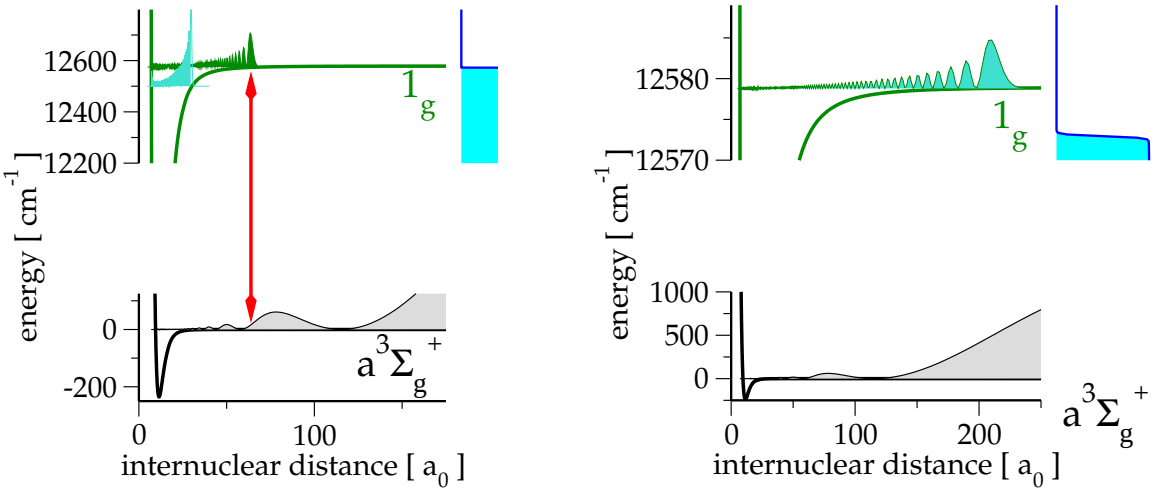

FIG. 1: In one-photon photoassociation, blocking the spectral amplitudes at and close to the atomic resonance prevents weakly bound molecular levels with large free-bound Franck-Condon factors to be excited (right-hand side). The majority of spectral components does not find any ground state population to be excited since the probability to find two colliding atoms at short internuclear distance is tiny (left-hand side, data shown here for Rb_2). In femtosecond photoassociation employing a one-photon transition, the large majority

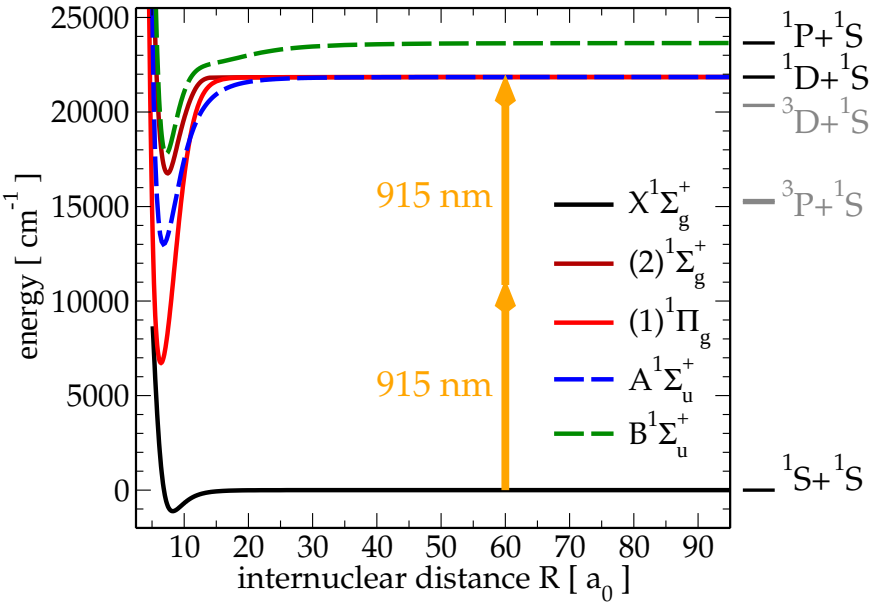

FIG. 2: Two-photon photoassociation of two atoms colliding over the $X^1\Sigma_g^+$ ground state into the $(1)^1\Pi_g$-state or the $(2)^1\Sigma_g^+$-state correlating to the $s+d$ asymptote (solid lines). The dipole coupling is provided by the states with one-photon allowed transitions from the ground state such as the $A^1\Sigma_u^+$-state or the $B^1\Sigma_u^+$-state (dashed lines). The example shown here is Ca_2.

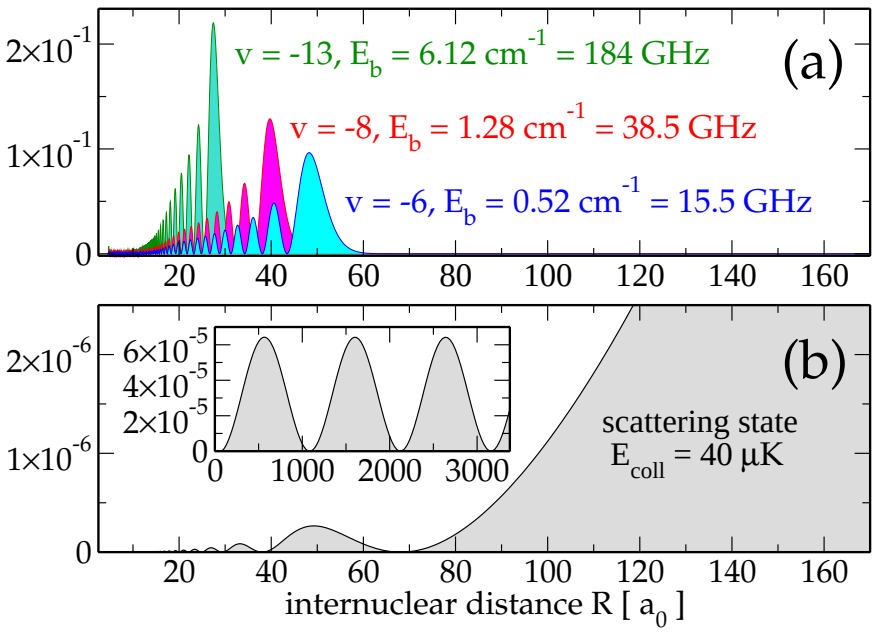

FIG. 3: Weakly bound vibrational wavefunctions of the $(1)^1\Pi_g$ excited state for three different binding energies relevant for photoassociation (a) and scattering wavefunction of two ground state calcium atoms (b).

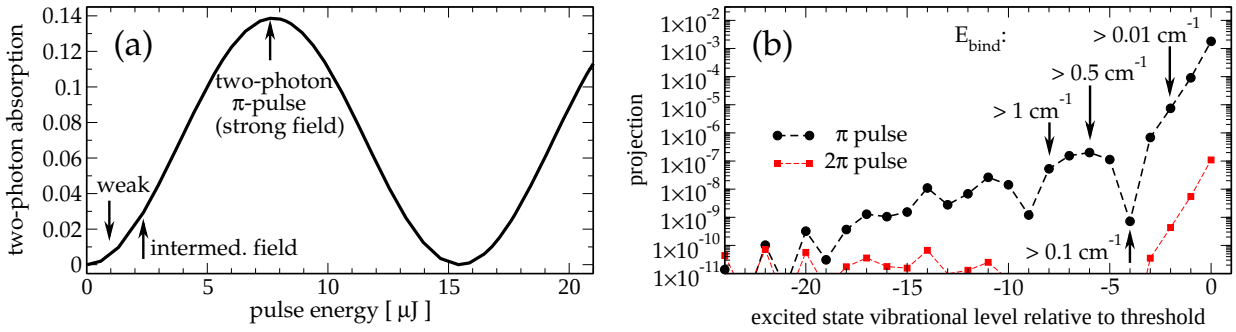

FIG. 4: (a) The excited state population shows Rabi oscillations as the pulse energy is increased. The arrows indicate the pulsed energies which are employed for shaped pulses. (b) The projection of the final excited state wave packet onto the molecular levels, i.e. the excited state vibrational distribution after the pulse for a two-photon π-pulse and a two-photon 2π-pulse. The arrows indicate the range of binding energies relevant in the discussion of the results for shaped pulses.

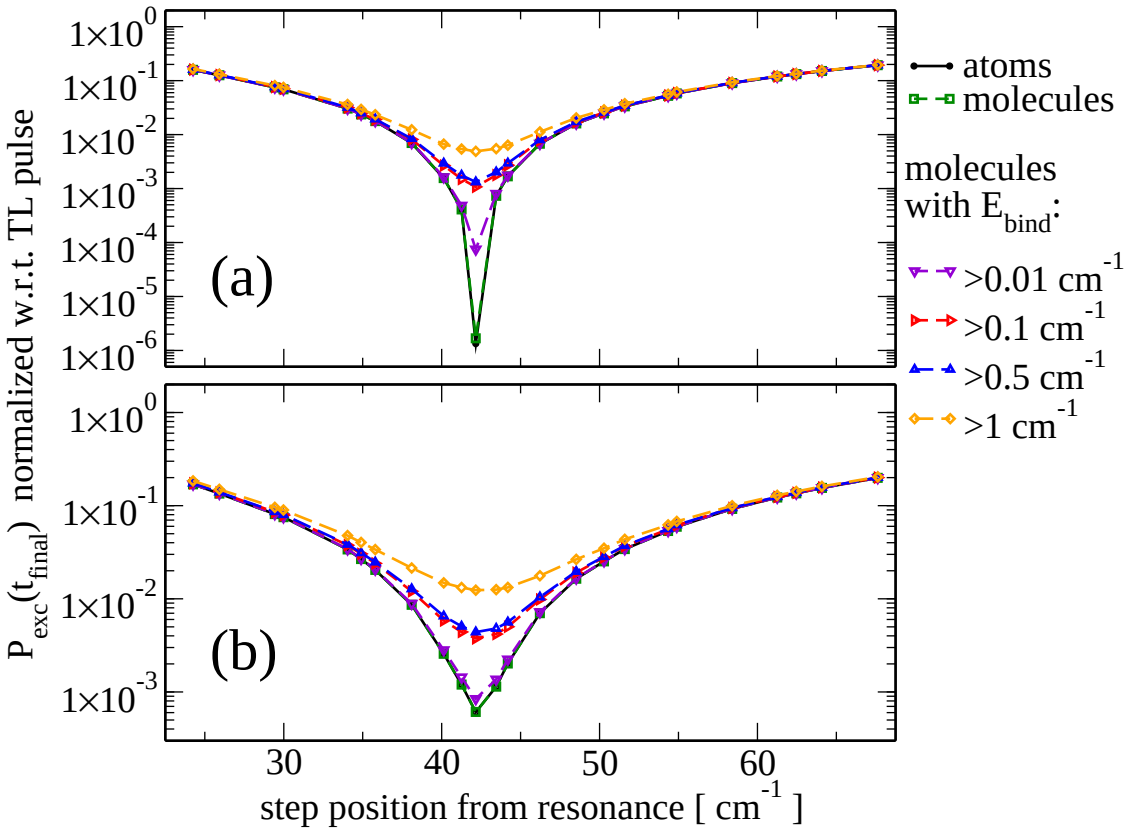

FIG. 5: Frequency-domain control with pulses shaped according to Eq. (11): The excited state population of atoms (filled circles) and of molecules (open symbols), normalized with respect to the results obtained for a transform-limited pulse, is shown as a function of the π-step position for (a) weak and (b) intermediate fields. Population transfer can be strongly suppressed, by 10^{-6}, for the weak field (a). For the intermediate field (b), the dynamic Stark shift sets in yielding a maximum suppression on the order of 10^{-3}. When all molecular levels are considered, the last two levels (that have binding energies of less than $0.01\,\mathrm{cm}^{-1}$) dominate and no difference between atoms and molecules is observed. For increasing binding energy of the molecular levels, and hence detuning from the atomic resonance, the two-photon transition becomes less dark.

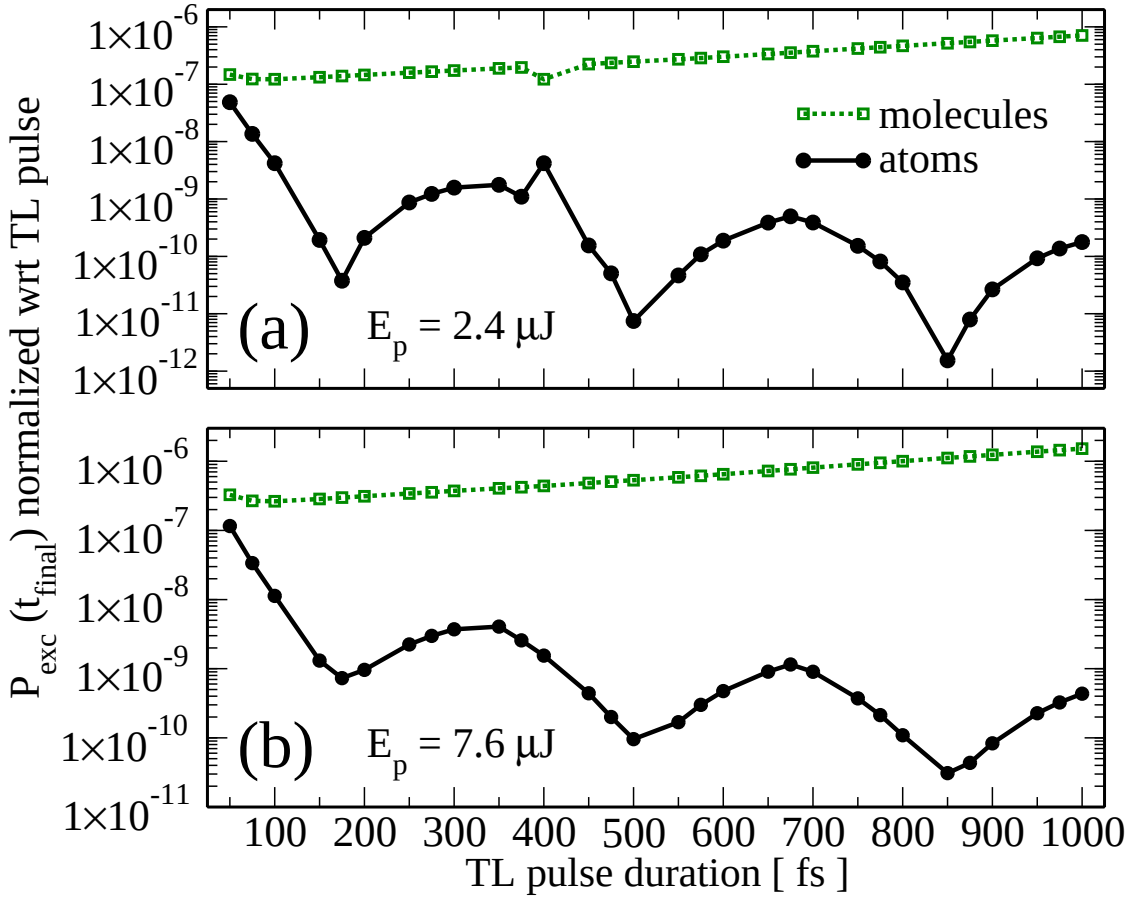

FIG. 6: Time-domain control with pulses shaped according to Eq. (16): The excited state population of atoms (filled circles) and of molecules (open symbols), normalized with respect to the results obtained for a transform-limited pulse, is shown as a function of the duration of the corresponding transform-limited pulse for intermediate (a) and strong field (b). Two-photon transitions for atoms are more strongly suppressed than for molecules. However, the suppression of the molecular transitions is too strong to achieve any significant photoassociation yield. For weakly bound levels no difference in the suppression with increasing binding energy is observed, i.e. the levels have very similar dynamic Stark shifts.